Submitted to Applied Physics Letters on 6th Feb 01 2167

Non-reciprocal transmission in a direct-bonded photorefractive Fe:$LiNbO_3$ buried waveguide

Corin B. E. Gawith, Ping Hua, and Peter G. R. Smith

Optoelectronics Research Centre

University of Southampton

Southampton

SO17 1BJ, UK

Email: cbeg@orc.soton.ac.uk

Gary Cook

Defence Evaluation and Research Agency

St. Andrews Road

Great Malvern

Worcestershire

WR14 3PS, UK.

Abstract

We report the fabrication of a 20-μm-thick photorefractive Fe:$LiNbO_3$ planar waveguide buried in MgO:$LiNbO_3$ by direct bonding of precision polished surfaces. Non-reciprocal transmission measurements were performed in a 3-mm-long device with a cw 532 nm frequency-doubled YAG laser source. A Fresnel reflection based counter propagating beam arrangement was used to measure a relative change in optical density (ΔOD) of approximately 2 within the waveguide, with a photorefractive response time of 4-5 milliseconds.

Non-reciprocal transmission can occur when two counter-propagating beams couple through a reflection grating in certain photorefractive crystals [1,2]. As the two beams interfere in the photorefractive media, charges excited from the bright fringes diffuse into the dark fringes, creating a periodic charge distribution throughout the illuminated region and an associated periodic electric space-charge field. This in turn causes a change in the refractive index of the material through the linear Pockel's effect, creating a refractive index grating that is phase shifted (ideally by 90 degrees) with respect to the light interference pattern and allowing energy to be coupled from one beam to the other [2]. Power transfer occurs in one direction only, leading to reduced power transmission in one direction and increased power transmission in the opposite direction, as determined by the sign of the effective electrooptic coefficient of the crystal.

A primary application of this effect is optical limiting, where a crystal is used to reduce the transmission of coherent laser light while continuing to transmit incoherent light. This has recently received considerable attention as a means of achieving rapid optical limiting of low power continuous wave (cw) lasers, necessitating the development of efficient photorefractive materials and devices. An important material in this respect is iron-doped lithium niobate (Fe:$LiNbO_3$), a photorefractive crystal featuring an exceptionally high optical small signal gain coefficient of up to 100 cm^{-1} [3]. This high gain coefficient, together with the use of a simple focal plane geometry, has led to reported changes in optical density (ΔOD) of up to 4 with 1/e switching speeds of a few milliseconds [3]. At small system apertures (f/20 or smaller) bulk Fe:$LiNbO_3$ crystals have been found to work exceedingly well in a focal plane geometry. However, at wider apertures where the confocal parameter

becomes less than the crystal path length, the degree of optical limiting decreases rapidly, becoming negligible towards large apertures, e.g. f/1 [4]. This effect is thought to arise from competition with dark conductivity in the lower-intensity areas away from the beam waist, which reduces the effective optical interaction length within the Fe:$LiNbO_3$ crystal [4]. An ideal solution is therefore to replace the bulk crystal with a photorefractive optical waveguide in which the interaction length can be made arbitrarily long and the focussed intensity is no longer related to the effective interaction length [4].

To this end, this letter describes our initial study towards producing an Fe:$LiNbO_3$ photorefractive waveguide device buried in MgO:$LiNbO_3$ by direct bonding (DB) [5,6] and precision polishing techniques. Previously applied methods of waveguide manufacture in this material, such as mechanical sawing [4,7], proton exchange [4] and light induced frustrated etching (LIFE) [4,8], have resulted in high losses, no optical limiting, and undersized features, respectively. By contrast, direct bonding is a fabrication technique used to create low-loss, seamless, vacuum tight bonds between dissimilar material layers, and has been previously used in the design and realisation of highly efficient lithium niobate waveguide devices [9]. Here, the combination of a photorefractive Fe:$LiNbO_3$ waveguide with direct-bonded non-photorefractive MgO:$LiNbO_3$ cladding layers has resulted in an efficient buried waveguide device for optical limiting experiments.

Fabrication of the waveguide device began with a sample of $LiNbO_3$ doped with 0.08 molar % of iron. Provided that the crystal has a sufficiently high electron-trap density, optical limiting in Fe:$LiNbO_3$ is insensitive to the total Fe content (at least

over the doping range of 0.01 molar % to 0.1 molar %) and depends mainly on the linear transmission characteristics of the crystal which in turn depend on the relative densities of the Fe^{2+} and Fe^{3+} oxidation states of the iron doping. In Fe:$LiNbO_3$, the Fe^{2+} ions absorb in the visible spectrum and act as electron charge donors, while the Fe^{3+} ions are transparent and act as charge traps. A linear transmission of between 30 % and 60 % in uncoated crystals with 3 mm to 6 mm path lengths usually gives good results [2]. Magnesium-doped lithium niobate (MgO:$LiNbO_3$) was chosen for both the substrate and cladding layers of our buried waveguide device. MgO:$LiNbO_3$ has a refractive index lower than that of either undoped lithium niobate or Fe:$LiNbO_3$ [10] and features similar thermal properties to those of the iron-doped waveguide layer, an important prerequisite when annealing bonds at high temperatures. An additional benefit of MgO:$LiNbO_3$ is that the MgO doping effectively suppresses the photorefractive effect, ensuring that non-reciprocal transmission will be observed in the buried waveguide region of our device only. For this experiment 5 molar % of magnesium was added to the melt during crystal growth, a value associated with photorefractive resistance in lithium niobate [11].

From each crystal type a 1-mm-thick x-cut substrate of 6 mm × 6 mm surface area was diced and polished to provide an optically flat surface suitable for DB. After cleaning, a mixture of H_2O_2-NH_4OH-H_2O (1:1:6), followed by several minutes of rinsing in deionised water, was applied to both materials in order to render their surfaces hydrophilic [12]. The Fe:$LiNbO_3$ and MgO:$LiNbO_3$ layers were then brought into contact at room temperature, with both samples aligned along the same crystalline orientation, and finger pressure applied in order to promote adhesive avalanche [13]. This effect forces any excess air or liquid from between the two substrates, as

demonstrated by the elimination of the interference fringes at the crystal interface. Annealing of the bonded sample at 350 °C for 6 hours provided a sufficient bond strength for further machining and the Fe:$LiNbO_3$ region was then polished down to obtain a waveguiding layer of 20-μm-thickness (with a variance of less than 1 μm across the entire layer). A further cladding layer of MgO:$LiNbO_3$ was then added with the same procedure as above. The device was completed by removing any residual unbonded edge regions with dicing equipment and polishing the end faces of the waveguide to a parallel optical finish. The final dimensions of the buried Fe:$LiNbO_3$ waveguide device are given in Figure 1.

Measurement of non-reciprocal transmission in our Fe:$LiNbO_3$ waveguide was performed using two-beam coupling in a counter-propagating beam geometry, a technique illustrated in Figure 2. This allows the signal beam to be derived from the weak Fresnel reflection of the incident beam at the exit face of the crystal [4], eliminating the need for beam splitters and other ancillary optics. The device is inserted into the beam such that the incident light propagates along the z-axis of the crystal, providing access to the material's highest effective electro-optic coefficient, $r_{eff} = \pm r_{13} \approx 9.6$ pm V^{-1} [2]. For this experiment a continuous wave 532 nm frequency-doubled Nd:YAG laser source was expanded and then focussed onto the front face of the buried Fe:$LiNbO_3$ waveguide with a well corrected f/5 spherical lens. While a cylindrical lens would be more appropriate for use with our planar waveguide, allowing reduction of beam divergence in the unguided direction and thus a more uniform beam intensity along the crystal length, a spherical lens was used in this experiment owing to the large aberrations present in our available cylindrical lenses. A fast-response shutter mechanism was used to block the pump beam prior to each

crystal exposure and a photodiode was used to measure the far-field transmission characteristics of the device. Upon exposure, the pump transmission in the waveguide declines due to the formation of a volume reflection grating in the photorefractive material as the pump and signal beams interfere. At high intensities (where the photogeneration rate is much greater than the erasure rate from the dark conductivity) optical limiting occurs with a response time inversely proportional to intensity such that the rate of decline is rapid at first but becomes progressively slower as the intensity declines at the rear of the device. This effect is demonstrated in the oscillograph of Figure 3. From the trace, the relative change in optical density obtained by optical limiting, ΔOD, is determined by the equation

$$\Delta OD = \log_{10}(Ip / Iss) \qquad (1)$$

where I_P is the peak transmitted intensity at time t = 0 and I_{SS} is the steady state transmitted intensity. For our arrangement, an input focussed intensity of approximately 80 kW cm^{-2} gave a calculated ΔOD of 2 and 1/e response time of 4-5 milliseconds in the Fe:$LiNbO_3$ buried waveguide. The intensity required to achieve millisecond order response times in our photorefractive waveguide was higher than expected from similar experiments with bulk Fe:$LiNbO_3$ crystals [2], indicating non-optimised launch conditions or a possible change in local material properties during the direct bonding process. Since optical limiting in Fe:$LiNbO_3$ is intensity dependent [2], the first of these problems is likely to arise from the spherical lens used to focus light into the waveguide. Beam divergence in the unguided plane will rapidly reduce the pump intensity with distance, followed by a subsequent decrease in the ΔOD. This deleterious effect would not occur in a channel waveguide geometry, as

could be realised, for example, by titanium indiffusing a parallel array of channel waveguides into the planar iron-doped substrate prior to DB.

Investigation of the material properties of our direct bonded sample was performed using a scanning electron microscopy (SEM) based compositional line profile analysis. This technique was used to measure the relative difference in iron and magnesium concentrations across the polished end face of our device, the results of which are given in Figure 4. The graph shows significant inter-diffusion of iron and magnesium ions across the two bonded interfaces of the sample, indicating ion-exchange between the atomically-contacted substrate layers. Such a change in chemical composition is due to the high-temperature annealing used in DB [14] and represents a possible degradation mechanism for the optical limiting efficiency of the Fe:$LiNbO_3$ waveguide layer. For example, reduced iron content leads to reduced photoconductivity, electron trap density and charge generation and recombination rates, reducing the coupling gain and slowing down the response time of the photorefractive material. Further, the presence of magnesium at the edges of the buried waveguide suppresses the photorefractive effect in these areas, reducing the active volume of the waveguide layer. This reduces the average two-beam coupling gain and increases the input intensity needed to achieve a given reduction in optical transmission. However, optimisation of material composition and annealing conditions should reduce these effects in future devices.

In conclusion, we have reported the successful fabrication of a 20-μm-thick photorefractive Fe:$LiNbO_3$ waveguide buried in MgO:$LiNbO_3$ by direct bonding and precision polishing techniques. Characterisation of optical limiting in this device was

performed using two-beam coupling in a counter-propagating beam geometry with a 532 nm cw frequency-doubled YAG laser source. For an input focussed intensity of approximately 80 kW cm^{-2} a relative change in optical density of 2 and a response time of less than 5 milliseconds were achieved using f/5 focusing optics. This result represents an efficient waveguiding structure allowing access to wide aperture imaging systems for high-speed optical limiting applications. Future devices based on this technology are likely to incorporate multiple-layer structures and linear arrays of titanium indiffused channel waveguides.

The Optoelectronics Research Centre is an interdisciplinary research centre supported by the Engineering and Physical Sciences Research Council (EPSRC). This work has been supported by a DERA funded CASE award.

References:

[1] A. Krumins, Z. Chen, and T. Shiosaki, Opt. Comm. **117**, 147 (1995).

[2] G. Cook, D. C. Jones, C. J. Finnan, L. L. Taylor, and A. W. Vere, SPIE Proc. **3798**, 2 (1999).

[3] G. Cook, C. J. Finnan, and D. C. Jones, Appl. Phys. B. **68**, 911 (1999).

[4] G. Cook, J. P. Duignan, L. L. Taylor, and D. C. Jones, SPIE Proc. **4106**, 230 (2000).

[5] J. Haisma, G. A. C. M. Spierings, U. K. P. Biermann, and A. A. von Gorkum, Appl. Opt. **33**, 1154, (1994)

[6] A. Plößl and G. Kräuter, Mat. Sci. Eng. **R25**, 1, (1999).

[7] S. Yin, A. V. Petrov, Y. Suzuki, and K. Shinoda, Optical Memory and Neural Networks **7**, 155, (1998).

[8] I. E. Barry, R. W. Eason, and G. Cook, Appl. Surface Sci. **143**, 328, (1999).

[9] C. B. E. Gawith, D. P. Shepherd, J. A. Abernethy, D. C. Hanna, G. W. Ross, and P. G. R. Smith, Opt. Lett. **24**, 481 (1999).

[10] J. Noda, M. Fukuma, and S. Saito, J. Appl. Phys. **49**, 3150, (1978).

[11] T. Volk, N. Rubinina, and M. Wohlkecke, J. Opt. Soc. Am. B. **11**, 1681, (1994).

[12] Y. Tomita, M. Sugimoto, and K. Eda, Appl. Phys. Lett. **66**, 1484, (1995).

[13] J. Haisma, G. A. C. M. Spierings, T. M. Michelsen, and C. L. Adema, Philips J. Res. **49**, 23 (1995).

[14] C. B. E. Gawith, T. Bhutta, D. P. Shepherd, P. Hua, J. Wang, G. W. Ross, and P. G. R. Smith, Appl. Phys. Lett. **75**, 3757 (1999).

Figure Captions:

FIG. 1: Schematic diagram of the direct-bonded Fe:$LiNbO_3$ buried planar waveguide device.

FIG. 2: Two-beam coupling in a counter-propagating beam geometry in Fe:$LiNbO_3$.

FIG. 3: Far field optical limiting in the Fe:$LiNbO_3$ buried waveguide at 80 kW cm^{-2} peak focussed intensity at 532 nm.

FIG. 4: Chemical composition versus distance across the direct-bonded interfaces of the device. The non-symmetrical diffusion profile arises as a result of the two annealing processes required to complete the three-layered device.

Figure 1 Corin B. E. Gawith Applied Physics Letters

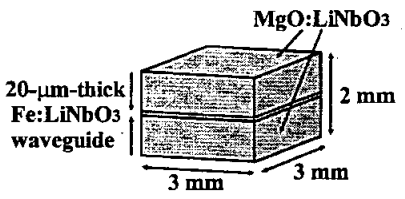

Figure 2 Corin B. E. Gawith Applied Physics Letters

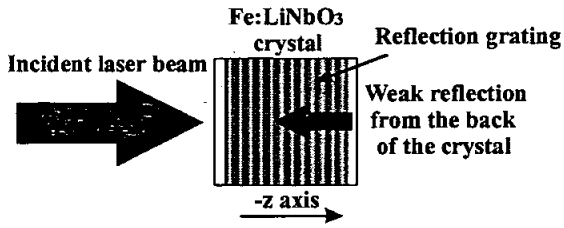

Figure 3 Corin B. E. Gawith Applied Physics Letters

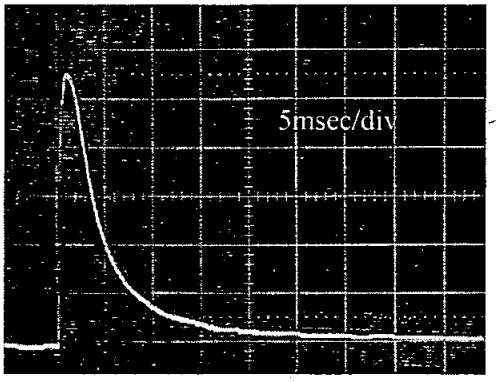

Figure 4 Corin B. E. Gawith Applied Physics Letters